

Direct Left Atrial Pressure Monitoring in Severe Heart Failure: Long-Term Sensor Performance

Richard W. Troughton · Jay Ritzema · Neal L. Eigler ·
Iain C. Melton · Henry Krum · Philip B. Adamson ·
Saibal Kar · Prediman K. Shah · James S. Whiting ·
J. Thomas Heywood · Spencer Rosero ·
Jagmeet P. Singh · Leslie Saxon · Ray Matthews ·
Ian G. Crozier · William T. Abraham ·
the HOMEOSTASIS Investigators

Received: 7 August 2010 / Accepted: 27 September 2010 / Published online: 14 October 2010
© The Author(s) 2010. This article is published with open access at Springerlink.com

Abstract We report the stability, accuracy, and development history of a new left atrial pressure (LAP) sensing system in ambulatory heart failure (HF) patients. A total of 84 patients with advanced HF underwent percutaneous transseptal implantation of the pressure sensor. Quarterly noninvasive calibration by modified Valsalva maneuver was achieved in all patients, and 96.5% of calibration sessions were successful with a reproducibility of 1.2 mmHg. Absolute sensor drift was maximal after 3 months at 4.7 mmHg (95% CI, 3.2–6.2 mmHg) and remained stable through 48 months. LAP was highly correlated with simultaneous pulmonary wedge pressure at 3 and 12 months ($r=0.98$, average difference of 0.8 ± 4.0 mmHg). Freedom from device failure was 95% ($n=37$) at 2 years and 88% ($n=12$) at 4 years. Causes of failure

were identified and mitigated with 100% freedom from device failure and less severe anomalies in the last 41 consecutive patients ($p=0.005$). Accurate and reliable LAP measurement using a chronic implanted monitoring system is safe and feasible in patients with advanced heart failure.

Keywords Heart failure · Hemodynamics · Implantable devices

Introduction

Despite advances in diagnosis and treatment, advanced heart failure (HF) is associated with high rates of decompensation, hospitalization, and death [1]. Implanted

R. W. Troughton · J. Ritzema · I. C. Melton · I. G. Crozier
Department of Cardiology, Christchurch Hospital,
Christchurch, New Zealand

H. Krum
The Alfred Hospital,
Melbourne, Australia

P. B. Adamson
Oklahoma Cardiovascular Research Group,
Oklahoma City, OK, USA

N. L. Eigler · S. Kar · P. K. Shah · J. S. Whiting
Cedars-Sinai Medical Center,
Los Angeles, CA, USA

J. T. Heywood
Scripps Hospital,
La Jolla, CA, USA

W. T. Abraham
The Ohio State University,
Columbus, OH, USA

J. P. Singh
Massachusetts General Hospital,
Boston, MA, USA

L. Saxon · R. Matthews
University of Southern California,
Los Angeles, CA, USA

S. Rosero
University of Rochester,
Rochester, NY, USA

R. W. Troughton (✉)
Department of Medicine, University of Otago,
PO Box 4345, Christchurch 8140, New Zealand
e-mail: Richard.Troughton@cdhb.govt.nz

cardiac filling pressure monitoring provides objective and continuous information on hemodynamic status in ambulatory HF patients that may facilitate the timeliness of interventions and improve outcomes [2–4]. A new permanently implanted left atrial pressure (LAP) monitoring system combined with a physician-directed patient self-management therapeutic paradigm improved the control of hemodynamics and reduced early clinical events in a small observational clinical study [5, 6]. This report describes the technical aspects of pressure sensor performance particular to long-term placement in the left atrium. Stability, accuracy, and causes of device malfunction are detailed and the effectiveness of modifications in sensor design and use to mitigate these problems are reported.

Methods

Implanted Sensor System

The implanted portion of the LAP monitoring system (HeartPOD[®], St Jude Medical, CRMD, Sylmar, CA) consists of an implantable sensor lead (ISL) and coil antenna (Fig. 1). The sensor module at the distal end of the lead has a hermetic titanium encapsulated pressure transducer that has four custom piezoresistive strain gauges affixed to the inside of a titanium diaphragm and integrated circuitry. The enclosure contains a helium/argon atmosphere. The sensor module is affixed to the atrial septum by proximal and distal folding nitinol anchors. The ISL is implanted during a transseptal catheterization performed from femoral or axillary/subclavian venous access. The implantation procedure began by performing a right heart catheterization with a Swan Ganz catheter. Transesophageal or intracardiac echocar-

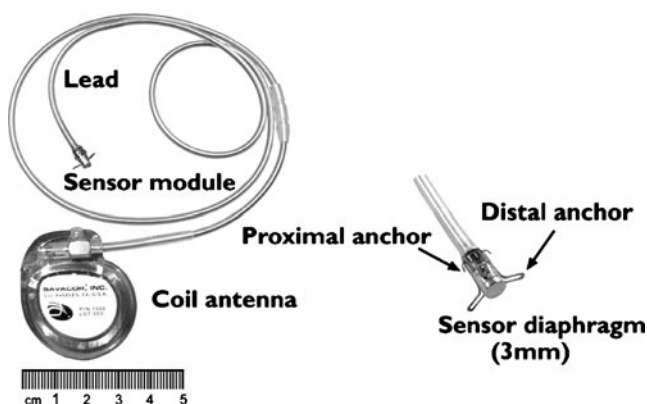


Fig. 1 *Left* Implantable left atrial pressure monitoring sensor lead and antenna coil. *Right* Close-up of the sensor module that is implanted in the atrial septum

diographic guidance at the time of the procedure or up to 1 week prior was used to confirm the absence of left atrial thrombus or atrial septal defect with more than a trace amount of intracardiac shunting. Transseptal puncture was performed using standard Brockenbrough needle/dilator techniques or with an experimental system that permitted left atrial cannulation from axillary venous access. After placing a guidewire in the left atrium, the patient was heparinized and an 11-F custom ISL delivery sheath was advanced across the atrial septum. The left atrial pressure was measured from the sheath and correlated with simultaneous pulmonary artery wedge pressure. The sensor was loaded into the delivery sheath with its anchors folded. The ISL was advanced until the sensor module exited the sheath in the left atrium. The sheath and ISL were withdrawn as a unit until the anchors engage the septum and were demonstrated to be secure. After removing the delivery sheath, the proximal lead connector was affixed to the antenna and placed in a subcutaneous pocket. In later cases, the proximal lead body was transferred from the femoral vein to axillary vein using custom-designed catheters.

A handheld Patient Advisor Module or PAM[®] device (Fig. 2) interrogates the sensor by placing the PAM in proximity (<5 cm) over the pocket. The PAM powers the sensor by 128 K-Hz radiofrequency induction and acquires digitally encoded LAP and atrial electrogram waveforms and core temperature from the sensor using reflective impedance telemetry. The LAP waveform is recorded at 200 Hz for 15 s. The PAM is programmed with a series of device constants that are used to convert raw digital sensor output into pressure values in millimeters of mercury. These constants are characterized for each sensor during manufacturing. The standard algorithm used to compute mean LAP is the mean of all sampled time points in the waveform. Segments of the waveform with excessive changes induced by an arrhythmia, coughing, sneezing, or breath holding are automatically rejected. If <5 s of continuous valid waveform remains, the patient is instructed to remeasure LAP. Alternative algorithms are programmable if specific compensation is required. One of these algorithms allows the alteration of the sensor's gain constants if scaling errors are later detected. Another algorithm takes advantage of the relationship between waveform amplitude and mean LAP and is thus independent of sensor offset drift.

Study Design

HOMEOSTASIS was a prospective, multicenter, observational open-label registry comprising the first human use of the LAP monitoring system for the management of chronic severe heart failure. The trial was approved by the US Food



Fig. 2 Noninvasive calibration system and procedure. *Top* Patient advisor module (PAM) with atmospheric pressure reference transducer connected to the mouthpiece for airway pressure measurement during Valsalva maneuver. PAM display allows the patient to view effort during strain and subsequently displays Valsalva waveforms for acceptance. *Bottom* Valsalva waveforms uncalibrated and calibrated: LAP (green), airway pressure (yellow), differential pressure (white), measurement period (between red lines), offset drift (blue line)

and Drug Administration (IDE G050018) and by the institutional review boards associated with each center. All subjects gave written informed consent. Details of the study design, patient characteristics, and clinical safety and effectiveness endpoints for the first 40 patients have been published [5, 6]. These patients were studied in detail with follow-up Swan-Ganz[®] right heart catheterization (RHC) at 3 and 12 months to assess sensor accuracy and stability. Simultaneous pulmonary capillary wedge pressure (PCWP) and LAP waveforms were recorded during four physiological states: rest, Valsalva maneuver (VM), isometric stress (3-min hand grip), and following nitroglycerin. Wedge position was confirmed by a change in waveform between balloon inflation and deflation.

Subsequently, an additional 44 patients were implanted. The protocol in this phase differed in that the entry criteria included chronic atrial fibrillation and new catheterization methods were used to achieve implantation in the pectoral region. Lessons learned during early use also drove the implementation of a modified ISL anchoring system,

improved manufacturing quality testing, and expanded implanter training. These changes were employed in the last 41 consecutive patients (group 2). The mean follow-up of all 84 patients was 25 ± 19 (range 1–63) months.

Valsalva Calibration

Prior to study enrollment, all patients had to demonstrate ability to perform a VM maintaining an airway pressure ≥ 40 mmHg for 8 s. All sensors were initially calibrated at implant to match catheter measurements. Thereafter, a noninvasive VM-based calibration method was used at scheduled clinic visits (2, 6, and 12 weeks and then every 3 months). Patients forcefully exhaled into a mouthpiece connected to the PAM's reference transducer (Fig. 2). Cardiac filling pressures and airway pressure have been shown to equalize after 5 s of strain [7]. Any inequality represents pressure transducer offset error also known as drift. This error was used to recalibrate the sensor. Individual VM attempts were excluded according to prospectively established criteria: (1) electronic noise caused by excessive motion of the PAM's external antenna with respect to the implanted antenna coil; (2) LAP pulse pressure not diminished by $>50\%$, indicating the VM did not sufficiently raise intrathoracic pressure; and (3) failure of the LAP to track the airway pressure during strain, indicating that airway pressure was not equivalent to intrathoracic pressure. A minimum of three VMs were attempted for each calibration session, and the mean of the corrections was used to calibrate the LAP sensor.

Statistical Analyses

The authors had full access to the data. Data are presented as mean \pm standard deviation or 95% confidence intervals (CI) as indicated. Reproducibility of the VM offset correction was quantified as pooled intra- and inter-patient standard deviations. Pressure values were correlated using Pearson's correlation coefficient, and Bland–Altman plots were used to assess differences between measurement techniques. The paired differences between LAP and PCWP were further characterized by a random effects model, with patient as a random effect. Comparisons were by *t* test. Technical device failure was defined as sensor malfunction sufficient to preclude use for guiding HF therapy. Device anomaly was defined as a sensor malfunction that was compensated for by alternative algorithms, and the LAP data were used to guide therapy. The choice to use LAP to guide HF therapy is determined by each site's principal investigator. Freedom from device failure and anomalies were evaluated by the Kaplan–Meier product limit method with comparisons by the log-rank test.

Results

Calibration, Drift, Accuracy

LAP sensors were successfully implanted in all 40 (100%) initial subjects. There were 1,813 VMs attempted during 511 calibration sessions (3.5 ± 1.1 VMs attempted per session). The large majority of VMs (87.1%) were accepted for analysis. Rejected attempts included: 0.2% for excessive noise, 1.8% for failure to reduce the LAP pulse pressure, and 10.9% for tracking failure. All patients performed acceptable VMs and most patients (83%) performed successful VM on $\geq 75\%$ of attempts. Nine patients had 18 calibration sessions (3.5% of sessions) where no VM attempts were acceptable. Sensor offset was maintained at previously stable values, and no additional right heart catheterizations were required specifically to calibrate an implant. Reproducibility of the pooled offset standard deviation from VM calibration sessions within patients ranged from 0.6 to 2.2 mmHg, and the pooled offset standard deviation from all patients and sessions was 1.2 mmHg.

Figure 3 quantifies pressure sensor drift over 48 months of follow-up. Mean drift compared to initial baseline at implant was low, never exceeding 1.3 mmHg at any of the

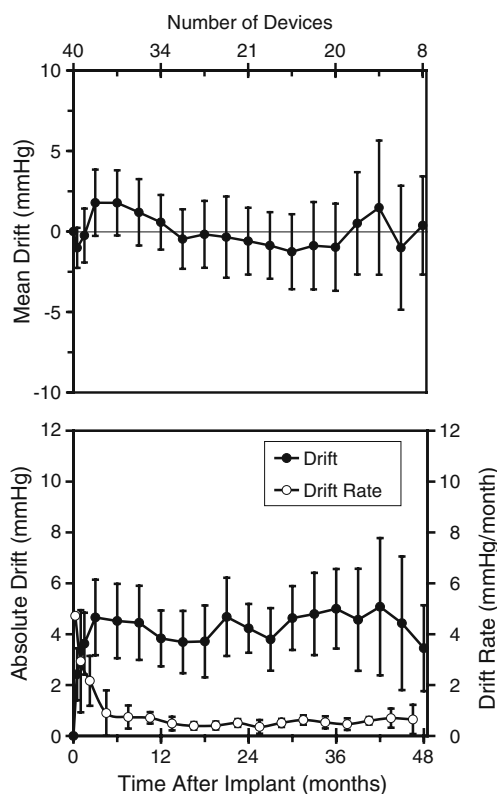


Fig. 3 Graphs showing mean drift, absolute drift, and drift rate as a function of time after implantation. Error bars=95% confidence intervals

quarterly measurement points. Absolute drift peaked after 3 months at 4.7 mmHg (95% CI, 3.2–6.2 mmHg) and remained stable through 48 months. Drift rate was highest during the first 2 weeks after implantation and then progressively declined by more than 80% after 6 months ($p=0.004$) and remained minimal and stable thereafter.

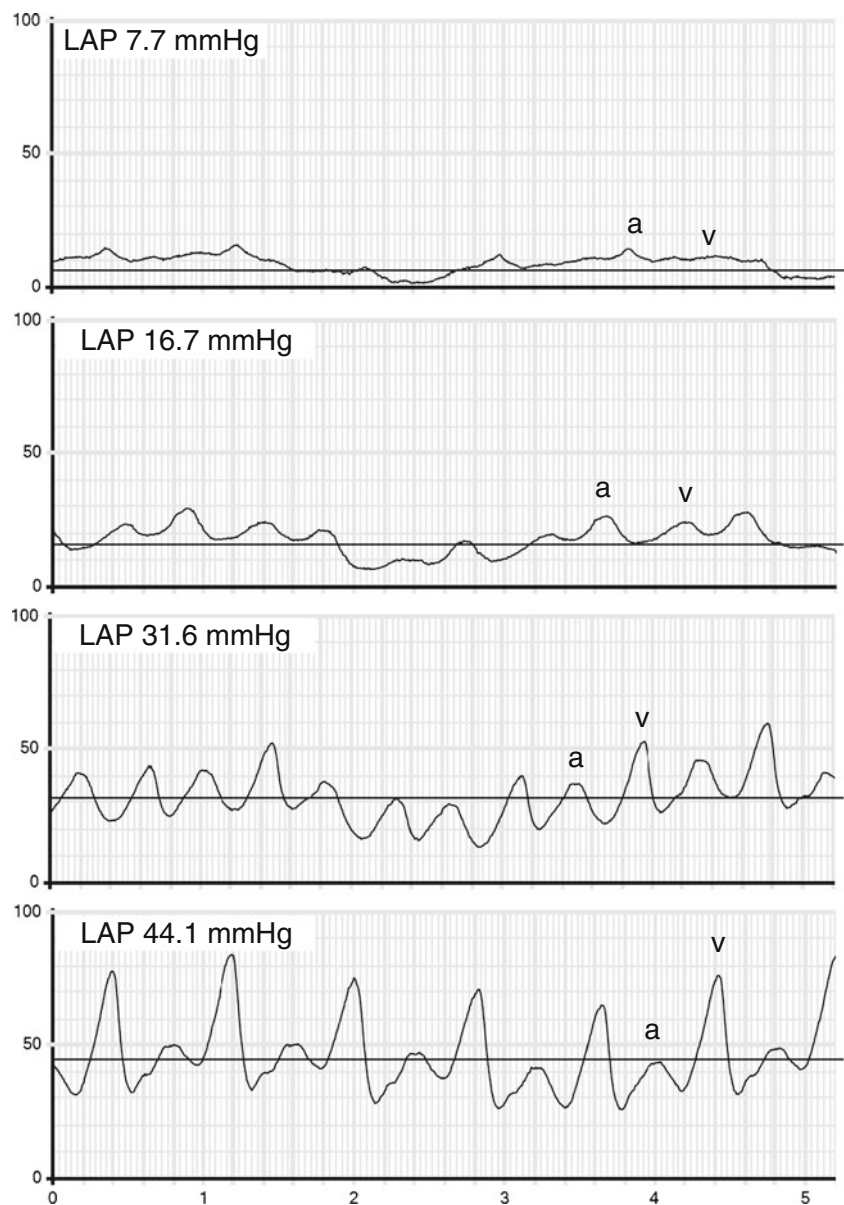
As shown in Fig. 4, the morphology of the LAP waveform showed characteristic changes with increasing LAP. In particular, the amplitude of the v-wave increased in concert with elevations in mean LAP. This relationship was seen in all patients with a normally functioning sensor and remained stable over the time course of the implant. In contrast, this characteristic increase in v-wave amplitude was not evident when waveform abnormalities were present. In patients with normal waveforms, the standard PAM algorithm (waveform mean) was compared to the traditional method of assessing the end-expiratory mean value between the peak of the a-wave and the beginning of the v-wave. If the patient was in atrial fibrillation, the end-expiratory 150-ms segment prior to onset of the v-wave was used instead. These methods were found to be highly correlated across patients with normally functioning sensors ($r>0.99$, difference= -0.4 ± 1.4 mmHg), across a wide range of pressures (1–61 mmHg), heart rates (up to 150 bpm) during atrial fibrillation, and respiratory variation (up to 30 mmHg).

Figure 5 compares LAP and PCWP in 32 of 40 patients with normal waveforms surviving long enough to have 3- or 12-month RHCs. The relationships were highly linear and the errors in estimating PCWP were small and did not show any trends.

Figure 6 examines the six patients that developed LAP waveform artifacts characterized as device anomalies. These artifacts were suspected by the investigators noting changes in waveform morphology and confirmed by marked differences (>5 mmHg) between the standard PAM algorithm and the traditional end-expiratory method. There was reduced agreement with PCWP, except for readings during a VM when filling pressures were >40 mmHg. PCWP was overestimated when v-waves were augmented and underestimated when v-waves were inverted. An automated compensatory algorithm based on the traditional algorithm modified as a fixed duration time window adjustable with respect to the R-wave of the left atrial electrogram significantly improved the correlation ($p<0.001$).

Figure 7 and Table 1 compare LAP with PCWP as a function of physiological state, pooled for all surviving patients and time points. LAP values were calculated by the standard PAM algorithm when waveforms were normal and by the modified traditional algorithm when artifacts were present. The two measures were highly correlated over a wide range of PCWP (0–98 mmHg), and differences between the methods were small (within ± 5 mmHg in

Fig. 4 LAP waveform from a single patient over a 10-day period. LAP values calculated from the mean of all points (*horizontal lines*). A-waves and v-waves confirmed from simultaneous electrograms (not shown)



80% of measurements). Measurement agreement was not altered by applying a mixed effects model to account for random effects of variation in the number of measurements between patients (0.8 ± 4.0 mmHg). When Valsalva comparisons were excluded, the range of filling pressures was still broad (0–53 mmHg) and the agreement between LAP and PCWP remained excellent ($r=0.92$; difference= 1.1 ± 3.9 mmHg).

Device Failures, Waveform Anomalies, and Mitigating Actions

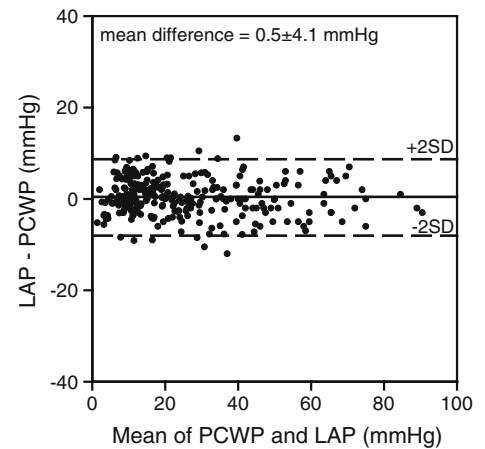
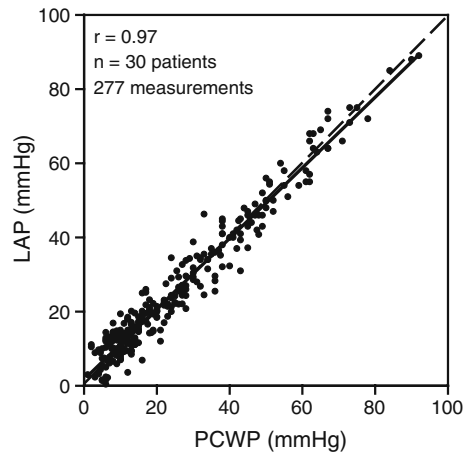
LAP sensors were successfully implanted in 82 of 84 (97.6%) subjects. During the first 4 years, six sensors met the criteria for device failure. One sensor had progressive

rapid drift developing after 26 months and two sensors had communication failures. Three sensors developed waveform artifacts that could not be sufficiently compensated for with alternative pressure measurement algorithms available in the PAM at that time. Freedom from device failure was 95% at 2 years and 88% at 4 years. There were 37 and only 12 non-failing devices available for review at 24 and 48 months, respectively. Three patients had a second ISL placed without difficulty, and in one of these patients, the non-working implant was extracted.

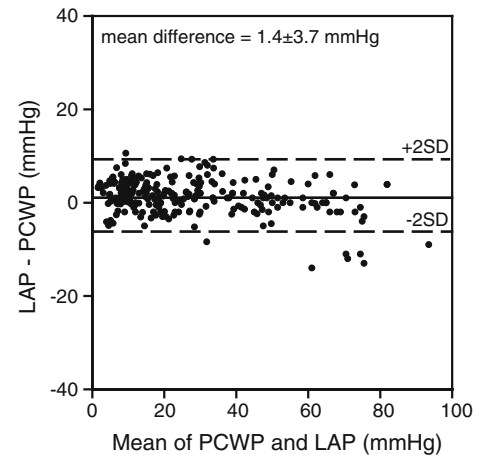
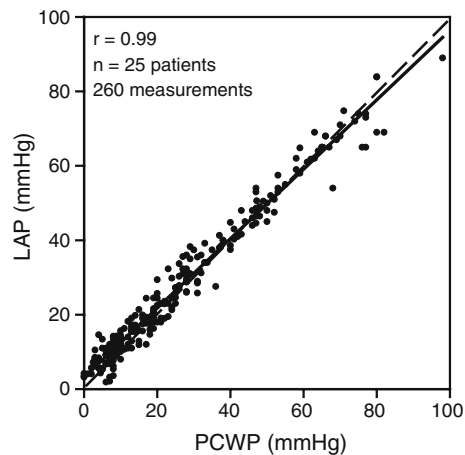
Less severe device anomalies not requiring sensor replacement were seen in eight patients. Two developed progressive rapid drift after 5 and 23 months, but were correctable either by repeat VM calibrations and the alternative offset-independent PAM algorithm. Six patients

Fig. 5 *Left* Scatter plots of left atrial pressure (LAP) vs. pulmonary capillary wedge pressure (PCWP) at 3 and 12 months after implantation. *Right* Bland–Altman plots showing differences between LAP and PCWP as a function of the mean of both pressure measurements at 3 and 12 months after implantation. All patients had normal (artifact-free) waveforms

3 Months



12 Months



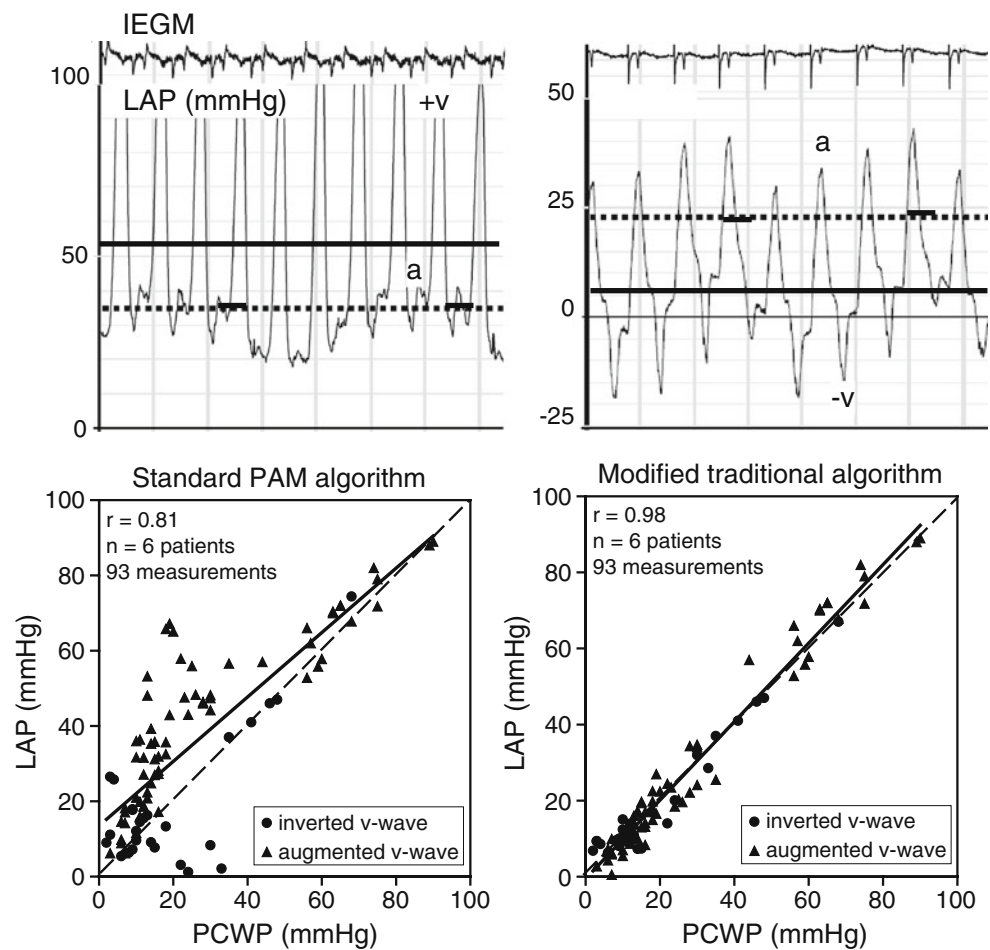
developed waveform artifacts that were satisfactorily compensated for by the alternative algorithms.

There were no instances of device failure or anomaly associated with clinical worsening. Figure 8 shows freedom from device failure or anomaly based on the type of abnormality observed and the effect of corrective actions. Excessive drift or device communication malfunctions were distributed throughout the follow-up period. The majority of devices (eight of nine) that developed waveform artifacts did so within the first 4 months after implantation.

The causes of progressive rapid drift and communication failures were determined and mitigated by improved quality testing during manufacturing. Animal testing and postmortem examinations determined that waveform artifacts were caused by excessive neoendocardial formation over the sensor diaphragm. Sensors tilted more than 45° from orthogonal to the atrial septum tended to develop enhanced a-waves and/or inverted v-waves at higher filling pressures ($n=6$). In three of these cases, devices were implanted through patent foramen ovale (PFO) tunnels witnessed by

blunt crossing during transeptal catheterization. These artifacts were associated with very thick tissue adherent to one side of the sensor diaphragm. In three cases with v-wave augmentation, sensors were more orthogonal and were symmetrically covered with thick tissue overgrowth. When the sensor diaphragm was covered by tissue, its motion reflects changes in atrial wall tension in addition to fluctuations in left atrial fluid pressure. Traditional end-expiratory measurement of LAP was reliable in the presence of waveform artifacts, possibly because these measurements were constrained to time points when wall tension was minimal. To mitigate waveform artifacts, implanting physicians have been trained to avoid placing devices via PFOs and a modified sensor anchoring system (Fig. 9) was implemented. The design change advances the pressure sensing diaphragm by an additional 1.5 mm into the left atrium with the intention of minimizing tissue thickness over the sensor and decoupling it from contraction and stretching movements of the atrial wall. The effect of these changes and improved manufacturing controls are

Fig. 6 Upper LAP and electro-gram tracings in patients with LAP waveform artifacts. The *left-hand tracing* is from a patient with augmented v-waves and the *right-hand tracing* is from a patient with augmented a-waves and inverted v-waves. The *solid lines* are the standard PAM algorithm mean of the LAP waveform. *Dotted lines* are the end-expiratory mean between the peak of the a-wave and the beginning of the v-wave (*hash marks*). *Bottom* Scatter plots comparing LAP and PCWP for patients with v-wave artifacts using standard PAM and the modified traditional algorithms to calculate mean LAP



measurable. The last 41 implants (group 2) have been free of artifacts, rapid progressive drift, and communication failures (log-rank $p=0.005$).

Discussion

Sustained elevations of LAP have long been recognized to be the proximate cause of cardiogenic pulmonary congestion because LAP is the dominant hemodynamic force causing intravascular fluid transudation into the pulmonary interstitium [8]. The potential clinical utility of permanently implanting pressure sensors for guiding heart failure therapy by controlling LAP has been demonstrated in several studies using early generation devices [2–6]. To be clinically acceptable, these devices will need to demonstrate sufficient safety and effectiveness in well-designed randomized trials. In addition, success also requires that these devices meet rigorous technical standards for diagnostic accuracy, stability, long-term functioning, and reliability [9]. Despite the promise of implantable hemodynamic monitoring, clinical trials have been halted precisely because of technical issues affecting device reliability [10,

11]. Moreover, addressing these issues requires a systematic effort to understand and correct the causes of sensor anomalies. This is the first report to chronicle the translational research particular to the evolutionary development of an implantable sensor that directly measures left atrial pressure.

Noninvasive Sensor Calibration

We previously showed in patients with existing heart failure that during phase II of a properly performed VM, all cardiac filling pressures equalize with airway pressure [7]. Put another way, the effective pressure gradient between the left atrium and the thorax is eliminated during VM. We postulated that deviations from this equality can be used to recalibrate sensor offset drift. The current study prospectively applied this observation as a new automated method to directly measure drift and recalibrate permanently implanted intracardiac pressure sensors.

VM calibration is advantageous because it is completely noninvasive and sensor drift can be accurately measured as frequently as required. VM calibration was well tolerated and together with assessment of LAP trends and waveforms

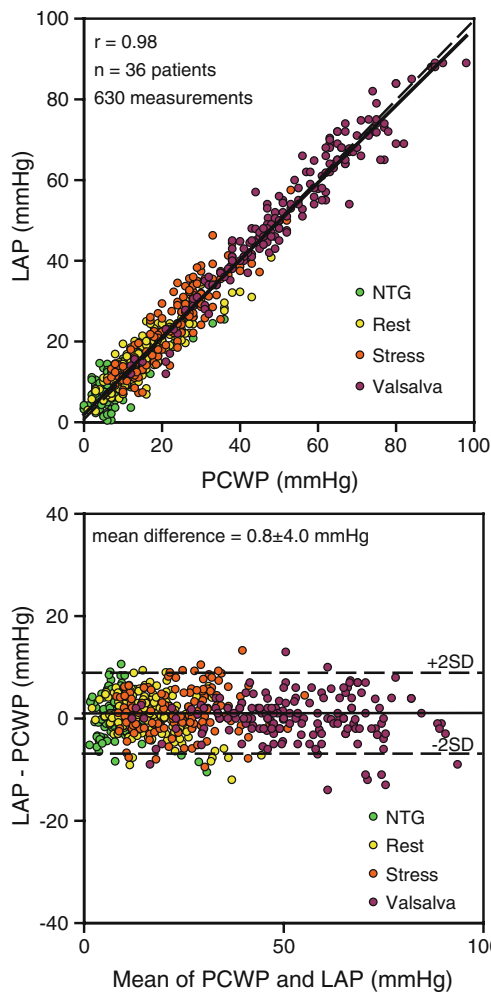


Fig. 7 Scatter and Bland–Altman plots comparing all simultaneous LAP and Swan–Ganz PCWP measurements at 3 and 12 months as a function of physiological state. LAP was calculated by the standard PAM algorithm in patients with normal waveforms and by the modified traditional algorithm in patients with waveform artifacts

Table 1 Simultaneous pressures from study device and Swan–Ganz catheter

	<i>n</i>	LAP	PCWP	Difference
3 months (35 subjects)				
Nitroglycerin	69	10.7±6.1	10.5±6.9	0.2±4.2
Rest	101	16.0±7.1	15.7±8.6	0.3±4.0
Isometric exercise	70	24.6±10.6	23.5±10.6	1.1±4.4
Valsalva	82	51.0±17.4	50.9±16.8	0.1±4.3
Overall	322	25.6±19.1	25.2±19.3	0.4±4.2
12 months (30 subjects)				
Nitroglycerin	71	10.0±4.8	8.2±5.6	1.7±3.3
Rest	94	16.6±8.0	15.0±8.5	1.6±3.0
Isometric exercise	58	25.2±11.3	23.0±10.1	2.1±4.2
Valsalva	85	53.4±17.4	53.3±18.4	0.1±4.2
Overall	308	26.9±20.6	25.6±21.4	1.3±3.8

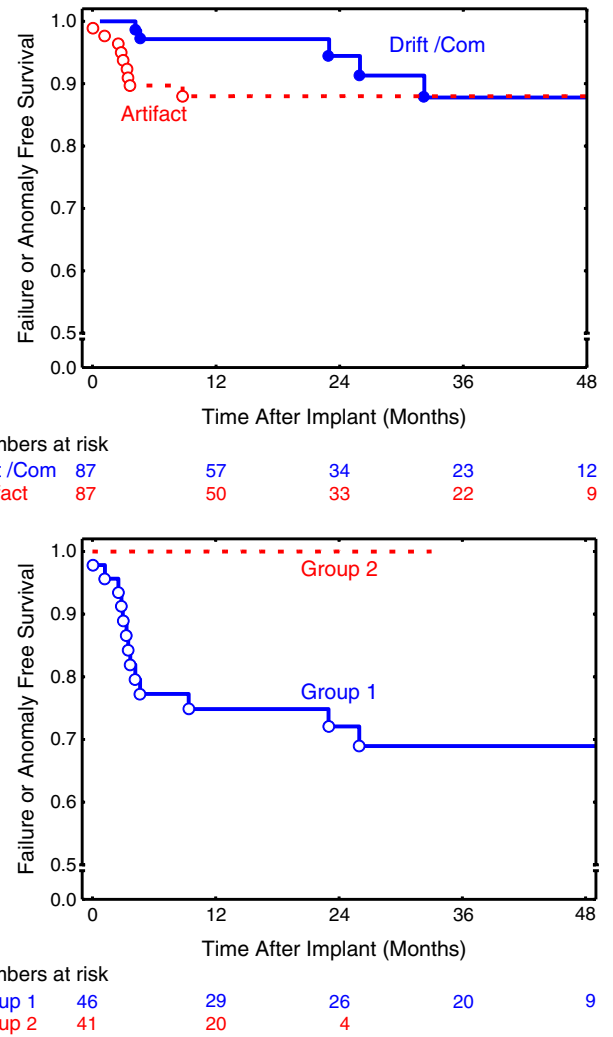


Fig. 8 *Top* Kaplan–Meier analysis showing the time course for the development of waveform artifacts compared to devices that developed rapid progressive drift or communication failures. *Bottom* Kaplan–Meier analysis of freedom from device failure or anomaly. Group 1 comprises consecutive devices 1 through 46 and group 2 are devices 47 through 87

generally required <15 min. VM calibration sessions were highly successful (96.5%) at yielding acceptable data and repeat VMs were highly reproducible with a pooled standard deviation of 1.2 mmHg.

Studies using other types of implanted pressure sensors have quantified mean sensor drift only at times of routine follow-up RHC [12, 13]. These studies may have missed early drift during the sensor healing period. The commonly used method of reporting drift as an arithmetic mean minimizes true changes because drift tends to be isotropic, having no preferential direction. When we quantified absolute changes from baseline, it was apparent that there were frequent small changes (around 5 mmHg) in sensor calibration during the first 6 months after implant and thereafter the drift became minimal out to 48 months. Drift

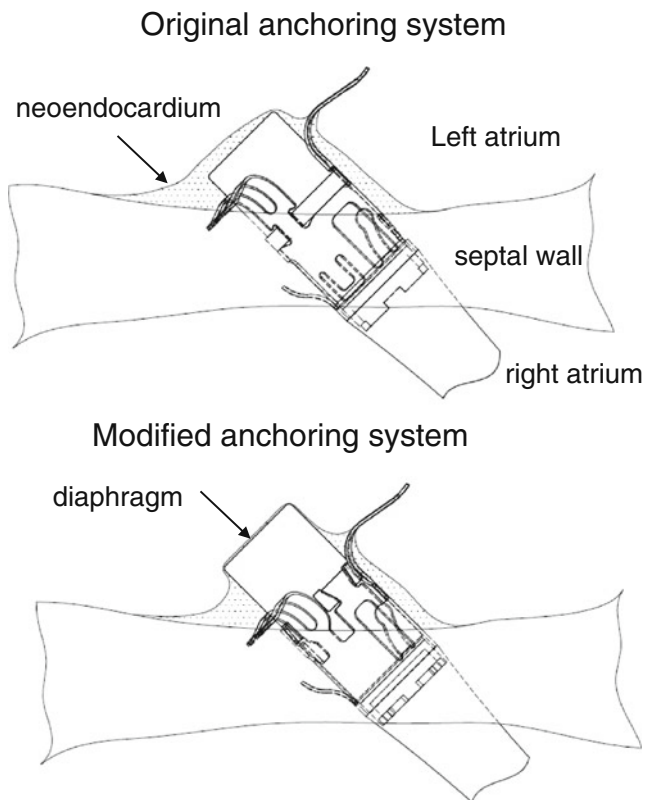


Fig. 9 Mechanism of waveform artifacts. *Top* Drawing showing original anchoring system used in group 1. When the sensor is angulated 45° from orthogonal to the atrial septum, the diaphragm develops asymmetrical neoendocardial overgrowth such that stretching of the atrial wall during filling pulls the diaphragm outward, creating an inverted v-wave. *Bottom* Modified anchor system used in group 2 implants. Increased protrusion of the diaphragm discourages thick tissue overgrowth and decouples the sensor diaphragm from the atrial wall, preventing waveform artifacts

that occurs early and then stabilizes is consistent with the time course of neoendocardial tissue coverage of the sensor. Also, the VM method successfully kept marginally functioning sensors sufficiently calibrated for long-term clinical use.

Comparative Hemodynamics

In this study, comparisons of LAP with PCWP generally showed a high degree of concordance. Although differences between LAP and PCWP >5 mmHg were seen in 20% of readings, the cause of any given discordance was not ascertained, nor did these differences prevent LAP measurements from successfully guiding therapy [5, 6]. One half of the discordant readings were concentrated in eight subjects where the intra-patient disagreement was entirely positive or entirely negative. These systematic errors likely result from miscalibration of the Swan Ganz catheter, the implanted LAP sensor, or both measurement systems. RHC measurements may be offset if the catheter/transducer

system is incorrectly “zeroed” or if the transducer height is not set to the level of the left atrium. Systematic measurement differences could also represent true physiological variances that have been documented particularly in patients with mitral valve disease or increased pulmonary vascular resistance [14, 15]. In the remaining patients, the errors were of similar propensity in either direction, suggesting more random variation. These errors may have been related to well-known variations in PCWP readings associated with under- or over-wedging of the balloon catheter or west zone effects [16]. The forementioned vagaries notwithstanding the comparison of LAP measured by a permanently implanted sensor, periodically calibrated using the VM method, were as accurate and reproducible as any comparison of simultaneously measured LAP and PCWP pressures obtained during cardiac catheterization studies [14, 15, 17–19].

Implanted sensors that measure surrogates for LAP including pulmonary artery diastolic pressure (PAD), or estimate PAD from the right ventricular pressure tracing, may be limited by measurement errors that may be amplified in the presence of LV dysfunction and increased pulmonary vascular resistance [20, 21]. Megalski et al. [12] reported that right ventricular pressure sensor estimates of PA diastolic pressure were correlated with simultaneous Swan–Ganz measurements of PA diastolic pressure ($R=0.84$, difference $\approx 2 \pm 7$ mmHg). Verdejo et al. [13] reported similar agreement between PA diastolic pressures measured by a wireless PA sensor compared with catheter pressures ($R = 0.69$, difference = -1.6 ± 6.8 mmHg). Neither study made comparisons with direct LAP or PCWP where additional errors would have been expected.

This first human experience with an implanted left atrial pressure sensor uncovered several technical issues affecting long-term implanted sensor performance. Suboptimal sensor performance was documented during early cases and was classifiable by type and severity. Intrinsic sensor malfunction included rapid progressive drift which was tracked down to hermetic leaks, and communication failure was caused by a physical defect in the internal electronic circuitry. Extrinsic causes of device abnormality were related to device positioning and healing with neoendocardial tissue coverage of the sensor. The more severe abnormalities precluded the clinical use of the device, and for less severe issues, compensatory actions were successfully implemented. Ideally, sensor failure and the need for individualized compensation should be rare.

Similar to coronary stenting, coverage of the bare metal sensor module with proliferating neoendocardium is desirable to prevent thrombus formation, but too much proliferation results in degraded sensor performance with waveform artifacts. Improvements to the sensor system design, manufacturing controls, and implantation techni-

ques were associated with the elimination of waveform artifacts and other causes of failure during limited follow-up in small numbers of patients. More and longer experience will be required to determine if these changes will successfully minimize failures and anomalies to clinically acceptable levels. More extensive experience is also required to detect if other less frequent but important device-related issues exist. These feasibility data, along with the implementation of the lessons learned now, warrant proceeding with adequately powered multicenter controlled randomized trials to evaluate the safety and effectiveness of this device-based heart failure therapeutic strategy.

Limitations

The current report is limited to a description of sensor performance over a median follow-up of 14 months. However, stable sensor performance was demonstrated for early devices out to 62 months at the time of reporting. The sensor measures direct left atrial pressure; however, comparison with invasive direct LAP measurements as a control was not feasible during follow-up and PCWP was used as a validated and reliable estimate of LAP.

Conclusions

In this small, observational first human experience, direct left atrial pressure monitoring with a novel implantable device was feasible and durable over a 4-year period. Noninvasive device calibration was achievable, reproducible, and seems to be important during the first year after implantation. High-fidelity LAP measurements were accurate and closely predicted PCWP over a 12-month period and were sufficiently reliable for clinical use, including daily hemodynamic assessment in ambulatory patients with severe HF. Iterations in sensor design and use mitigated early causes of reduced reliability.

Acknowledgments We thank the study coordinators for their hard work and attention to detail. The study was sponsored by St Jude Medical, CRMD, Sylmar California.

Ethical declaration The research reported in this manuscript complies with the current laws of the countries in which it was performed.

Disclosures Drs. Kar, Eigler and Whiting disclose a financial interest in the manufacturer of the study device. Drs. Abraham, Adamson, Heywood, Matthews, Melton, and Troughton report receiving honoraria or consulting fees from St Jude or other companies that manufacture devices. The other authors report no conflict.

Open Access This article is distributed under the terms of the Creative Commons Attribution Noncommercial License which permits any noncommercial use, distribution, and reproduction in any medium, provided the original author(s) and source are credited.

Appendix

The following centers and investigators participated in HOMEOSTASIS trial providing the study subjects included in this publication (listed in alphabetical order according to center): *Alfred Hospital, Melbourne, Australia*—J Aw, D Kaye, H Krum, T Walton; *Auckland City Hospital, Auckland, New Zealand*—R Doughty, J Stewart; *Cedars-Sinai Medical Center, Los Angeles, CA*—N Eigler, S Kar, R Makkar, PK Shah, R Siegel, J Whiting; *Christchurch Hospital, Christchurch, New Zealand*—I Crozier, J Lainchbury, I Melton, M Richards, J Ritzema-Carter, G Roper, R Troughton; *Massachusetts General Hospital, Boston MA*—J Singh, S Moore; *The Ohio State University, Columbus OH*—WT Abraham (Study Chairman), P Binkley, C Bush, G Cooke, D Feldman, D Hart, G Haas, A Hasan, M Houmsse, C Leir, C Love, R Magorien, R Mehta, B White; *Oklahoma Cardiovascular Research Group, Oklahoma City, OK*—P Adamson, M Harvey; *Scripps Clinic, La Jolla, CA*—T Ahern, T Heywood, A Johnson, M Price, R Schatz, C Stinis, P Teirstein; *University of Southern California, Los Angeles, CA*—L Saxon, R Matthews; *University of Rochester, Rochester NY*—S Rosario, L Chen.

Data and Safety Monitoring Board—B Greenberg (Chair), M Mehra, J McAnulty. Clinical Events Committee—M Klapholz (Chair), M Semigran, D Benditt.

References

- Rosamond, W., Flegal, K., Friday, G., Furie, K., Go, A., Greenlund, K., et al. (2007). Heart disease and stroke statistics—2007 update: A report from the American Heart Association Statistics Committee and Stroke Statistics Subcommittee. *Circulation*, *115*, e69–171.
- Yu, C.-M., Wang, L., Chau, E., Chan, R. H.-W., Kong, S.-L., Tang, M.-O., et al. (2005). Intrathoracic impedance monitoring in patients with heart failure: Correlation with fluid status and feasibility of early warning preceding hospitalization. *Circulation*, *112*, 841–48.
- Bourge, R. C., Abraham, W. T., Adamson, P. B., Aaron, M. F., Aranda, J. M., Jr., Magalski, A., et al. (2008). Randomized controlled trial of an implantable continuous hemodynamic monitor in patients with advanced heart failure: The COMPASS-HF Study. *Journal of the American College of Cardiology*, *51*, 1073–79.
- Adamson, P. B., Magalski, A., Braunschweig, F., Böhm, M., Reynolds, D., Steinhaus, D., et al. (2003). Ongoing right ventricular hemodynamics in heart failure: Clinical value of measurements derived from an implantable monitoring system. *Journal of the American College of Cardiology*, *41*, 565–71.

5. Ritzema, J., Melton, I. C., Richards, A. M., Crozier, I. G., Frampton, C., Doughty, R. N., et al. (2007). Direct left atrial pressure monitoring in ambulatory heart failure patients: Initial experience with a new permanent implantable device. *Circulation*, *116*, 2952–59.
6. Ritzema, J., Troughton, R., Melton, I., Crozier, I., Doughty, R., Krum, H., et al. (2010). Physician-directed patient self-management of left atrial pressure in advance chronic heart failure. *Circulation*, *121*, 1086–1095.
7. McClean, D., Aragon, J., Jamali, A., Kar, S., Ritzema-Carter, J., Troughton, R., et al. (2006). Noninvasive calibration of cardiac pressure transducers in patients with heart failure: An aid to implantable hemodynamic monitoring and therapeutic guidance. *Journal of Cardiac Failure*, *12*, 568–76.
8. Guyton, A. C., & Lindsey, A. W. (1959). Effect of elevated left atrial pressure and decreased plasma protein concentration on the development of pulmonary edema. *Circulation Research*, *7*, 649–57.
9. Potkay, J. A. (2008). Long term, implantable blood pressure monitoring systems. *Biomedical Microdevices*, *10*, 379–392.
10. Bennett, T., Kjellstrom, B., Taepke, R., Ryden, L., & for the Implantable Hemodynamic Monitor Investigators. (2005). Development of implantable devices for continuous ambulatory monitoring of central hemodynamic values in heart failure patients. *PACE*, *28*, 573–584.
11. Adamson, P. B., Conti, J. B., Smith, A. L., Abraham, W. T., Aaron, M. F., Aranda, J. M., Jr., et al. (2007). Reducing events in patients with chronic heart failure (REDUCEhf). Study design: Continuous hemodynamic monitoring with an implantable defibrillator. *Clinical Cardiology*, *30*, 567–575.
12. Magalski, A., Adamson, P., Gadler, F., Böehm, M., Steinhaus, D., Reynolds, D., et al. (2002). Continuous ambulatory right heart pressure measurements with an implantable hemodynamic monitor: A multicenter, 12-month follow-up study of patients with chronic heart failure. *Journal of Cardiac Failure*, *8*, 63–70.
13. Verdejo, H. E., Castro, P. F., Concepción, R., Ferrada, M. A., Alfaro, M. A., Alcaíno, M. E., et al. (2007). Comparison of a radiofrequency-based wireless pressure sensor to Swan–Ganz catheter and echocardiography for ambulatory assessment of pulmonary artery pressure in heart failure. *Journal of the American College of Cardiology*, *50*, 2375–82.
14. Verel, D., & Stentiford, N. H. (1970). Comparison of left atrial pressure and wedge pulmonary capillary pressure: Pressure gradients between left atrium and left ventricle. *British Heart Journal*, *32*, 99–102.
15. Hildick-Smith, D. J., Walsh, J. T., & Shapiro, L. M. (2000). Pulmonary capillary wedge pressure in mitral stenosis accurately reflects mean left atrial pressure but overestimates transmitral gradient. *The American Journal of Cardiology*, *85*, 512–515.
16. West, J. B., Dollery, C. T., & Naimark, A. (1964). Distribution of blood flow in isolated lung: Relation to vascular and alveolar pressures. *Journal of Applied Physiology*, *19*, 713–724.
17. Waltson, A., & Kendall, M. E. (1973). Comparison of pulmonary wedge and left atrial pressure in man. *American Heart Journal*, *86*, 59–64.
18. O’Quin, R., & Marini, J. J. (1983). Pulmonary artery occlusion pressure: Clinical physiology, measurement and interpretation. *The American Review of Respiratory Disease*, *128*, 319.
19. Lozman, J., Powers, S. R., Jr., Older, T., Dutton, R. E., Roy, R. J., English, M., et al. (1974). Correlation of pulmonary wedge and left atrial pressures: A study in the patient receiving positive end expiratory pressure ventilation. *Archives of Surgery*, *109*, 270–277.
20. Drazner, M. H., Hamilton, M. A., Fonarow, G., Creaser, J., Flavell, C., & Warner Stevenson, L. (1999). Relationship between right and left-sided filling pressures in 1000 patients with advanced heart failure. *The Journal of Heart and Lung Transplantation*, *18*, 1126–32.
21. Jenkins, B. S., Bradley, R. D., & Branthwaite, M. A. (1970). Evaluation of pulmonary arterial end-diastolic pressure as an indirect estimate of left atrial mean pressure. *Circulation*, *42*, 75–78.